Cholesteric spherical reflectors as innovative optical elements with vast application potential

Jan P.F. Lagerwall

Experimental Soft Matter Physics group, Department of Physics & Materials Science,
University of Luxembourg, 1511 Luxembourg City, Luxembourg

ABSTRACT

Cholesteric Spherical Reflectors (CSRs) are omnidirectional selective retroreflectors enabled by the ability of cholesteric liquid crystals (CLCs) to self-assemble with helicoidally modulated long-range orientational order, turning them into a liquid chiral photonic crystal with one-dimensional periodicity. The liquid state allows us to easily mold the CLC into spherical units, with stabilizers in the surrounding liquid phases ensuring the appropriate boundary conditions. By varying the composition of the CLC we can continuously tune the wavelength band of retroreflection across the visible spectrum and into the ultraviolet (UV) as well as infrared (IR) regimes, choose whether the CRSs reflect right- or left-handed circular polarization, and we can make them polymerizable, such that the CSRs are easily turned into solids after annealing, allowing easy manipulation and incorporation into diverse matrices. This opens for numerous innovative applications, from anti-counterfeiting and supply chain track-and-trace solutions, via human-invisible signage optimized for robots and AR device wayfinding, to the pixelation of structural color for generating non-spectral colors without absorption or indiscriminate scattering, and even enhanced-sensitivity disease testing. In my talk, I will briefly introduce the concept of CSRs and highlight their salient features, and then I will focus on our on-going efforts to solve important societally and industrially relevant problems by taking advantage of the opportunities offered by CSRs.

Keywords: Cholesteric liquid crystals, structural color, retroreflector, Bragg diffraction, anti-counterfeiting, fiducial markers

1. INTRODUCTION

The seemingly simple acts of molding a cholesteric liquid crystal (CLC) into a sphere, annealing it until the desired configuration of its self-assembled helical director configuration has been reached, and then polymerizing it into a solid have profound impact on the ability of applying the unique optical properties of CLCs, unleashing enormous potential for solving pressing problems across vast fields.[1–3] The cholesteric liquid crystal phase is a chiral version of the nematic phase. The fact that cholesterics belong to the class of nematics means that they exhibit long-range orientational order but no positional order of the molecules: the typically rod-shaped liquid crystal-forming molecules (mesogens) tend to align along a common direction referred to as the *director*, abbreviated **n**. In contrast to individual mesogens, which cannot be attributed optical properties in the traditional sense since they are two orders of magnitude smaller than visible light wavelengths (a fact that is frequently neglected in the modern scientific literature), the director is a continuum concept and it defines the (local) optic axis of the uniaxially birefringent nematic. With rod-shaped mesogens, the birefringence is positive, $\Delta n = n_{||} - n_{\perp} > 0$, where $n_{||}$ and $n_{\perp}$ are the refractive indices along and perpendicular to **n**, respectively, whereas the less commonly studied discotic cholesterics, due to their oblate mesogen shape, have $\Delta n < 0$.

The chirality of CLCs is manifested in the form of a helical modulation of **n** along a direction **m** that is perpendicular to **n**. Since **n** is also the local optic axis, this modulation implies a helically periodic modulation, with the pitch p of the helix, of the local refractive index for a particular linear polarization, turning the CLC into a one-dimensional chiral photonic crystal: circularly polarized light with the same handedness as the helix and a wavelength in the band $\Delta\lambda = \bar{n}p \pm (p\Delta n)/2$ cannot propagate along **m** but is instead selectively reflected,

Further author information:
E-mail: jan.lagerwall@lcsoftmatter.com, Telephone: +352 46 66 44 62 19

a phenomenon first elucidated by Oseen,[4] 18 years later analyzed in more detail by de Vries.[5] Here, $\bar{n}$ is the average refractive index in the CLC. The next milestone in the description of the optical properties of CLCs was provided by Fergason in 1966,[6] giving quantitative equations for the angle dependence of the selectively reflected color which consider variations in the orientation of the helix axis $\mathbf{m}$ as well as refraction at the interface between the CLC and its surrounding phase. For the case that the surrounding refractive index is matched to $\bar{n}$, which is the relevant case for applications of CSRs, we can ignore the refraction and then get for the central wavelength of the selective reflection band:

$$\lambda_r = \bar{n}p\cos\theta = \lambda_0\cos\theta. \tag{1}$$

Here θ is the incidence angle of light with respect to $\mathbf{m}$, and we define the retroreflection wavelength $\lambda_0 = \bar{n}p$, which is the maximum wavelength of selective reflection, occurring at $\theta = 0$, thus with light incidence parallel and reflection antiparallel to $\mathbf{m}$.

While droplets of liquid crystals were investigated already at the time of Lehmann's pioneering work,[7] among the first papers that raised the recent interest in spherically shaped CLCs was the demonstration by Humar and Musevic of omnidirectional lasing from dye-doped CLC droplets with radial $\mathbf{m}$.[8] Around the same time, the power of microfluidics for processing liquid crystals into droplets and shells was being recognized,[9] and my group joined this very active research field with much excitement. After initially working on non-chiral nematics and smectics, we presented our first paper on cholesteric droplets with selective reflection in the visible range in 2014, demonstrating that their peculiar optics go well beyond that of enabling omnidirectional lasing, particularly describing and explaining the intricate patterns that arise from photonic cross communication between cholesteric droplets assembled in a plane.[10] In the present paper I review our very active research in this field during the decade that has passed, initially focusing on elucidating the optics of CLCs molded into spheres, then gradually focusing more on making robust and easy-to-handle Cholesteric Spherical Reflectors (CSRs) by polymerizing liquid crystal shells and droplets without loss of the self-assembled order, and eventually exploring diverse application opportunities in collaboration with experts of each targeted field. After succinctly reviewing the key characteristics of CSR optics I will discuss a number of application scenarios that we have proposed during the last years.

2. THE UNIQUE OPTICS OF CHOLESTERIC SPHERICAL REFLECTORS

2.1 Photonic cross-communication

Under unidirectional white illumination, the spherical shape and radial orientation of $\mathbf{m}$ lead CSRs to selectively reflect light into a continuous set of cones, with reflection wavelength blueshifting with increasing cone angle,[10] as prescribed by Equation (1). This is illustrated in Fig. 1 for the case of reflections at the outside of a CSR with helix pitch giving rise to retroreflection at 650 nm, i.e., $\lambda_0 = \bar{n}p = 650$ nm. The cone opening angle, indicated in the figure together with the wavelength of maximum intensity in each particular light cone, is 2θ, i.e., twice the incidence angle with respect to the helix axis $\mathbf{m}$. The geometry means that $\mathbf{m}$ is oriented at an angle θ with respect to the direction of incident light at any point on the CSR surface. For $\theta = 0°$ to $\theta = 45°$ the cones are directed upwards and grow increasingly wider and flatter for increasing θ, while for $\theta > 45°$ the cones are directed downwards, growing narrower and less flat as θ increases further.

The borderline case of $\theta = 45°$ is particularly interesting as here the reflected light is in the horizontal plane. This means that if another CSR of the same type is found in that plane, that CSR will also reflect the light, and after this reflection the light will travel back to the original source, albeit with a lateral offset and a selection of a specific color, see Fig. 2. We termed this multi-CSR action on the same light ray *photonic cross-communication* in our original paper on the topic.[10] Since all CSRs in a sheet of CSRs engage in such cross communication and since they collectively send light fulfilling $\lambda_r = \bar{n}p\cos 45°$ back to the light source, we referred to this kind of retroreflection as *sheet retroreflection* in a more recent analysis that focused on the macroscopic behavior as observed at a distance from the sheet of CSRs.[11]

A key characteristic of the photonic cross communication is that it generates, at a microscopic scale, an intricate pattern that reflects the exact spatial arrangement of the CSRs in a sheet, as well as the design of each CSR in the sheet: considering only external reflections, colored spots appear in any CSR along radii in the plane of the sheet that point toward another CSR. Initially we assumed that all CSRs must exhibit identical optics

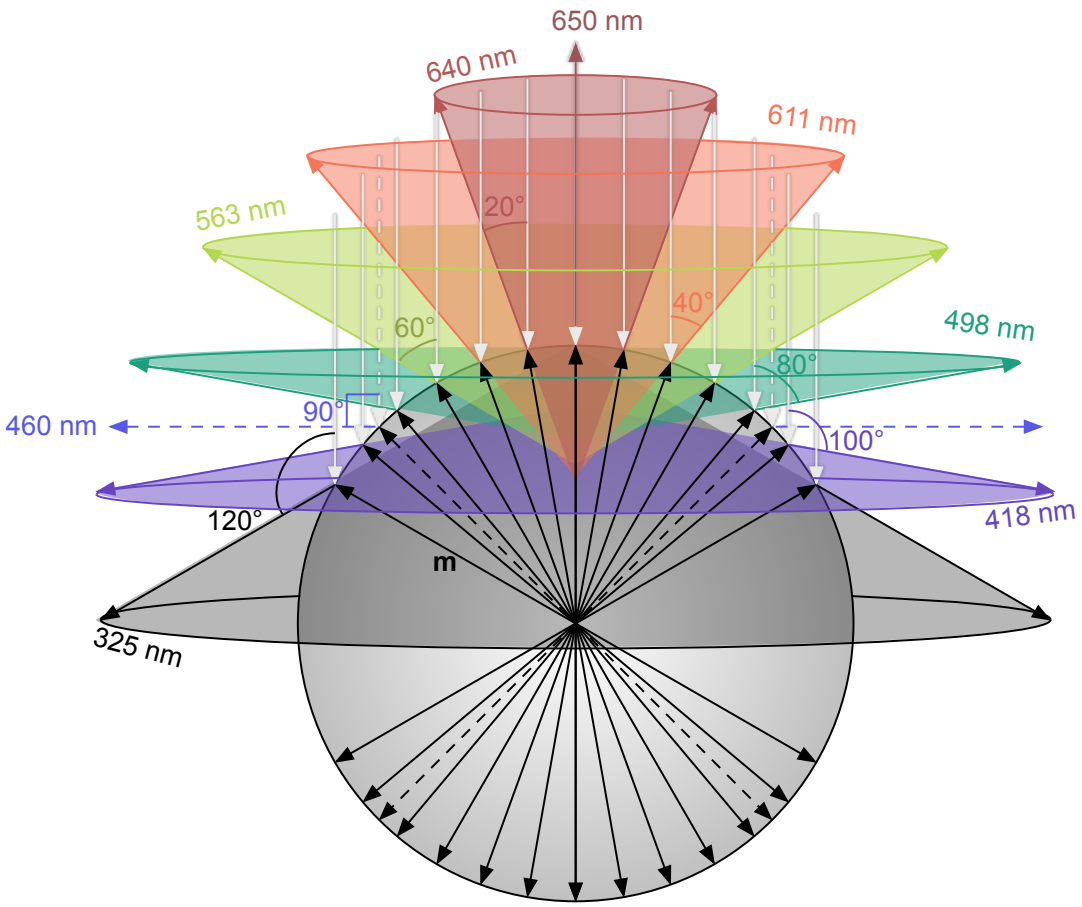

Figure 1. Schematic illustration of the cones of selective reflection of a CSR droplet. In all cases the illumination is with white light and vertical from above, as represented by grey arrows. Depending on where on the CSR a light ray hits, the fraction fulfilling the Bragg criterion is selectively reflected. At the top it is retroreflected with the maximum selective reflection wavelength λ_0. As the light hits further away from the center, it is reflected outwards, with increasing angle and increasing blueshift. Because of the spherical symmetry, each reflection color and direction is reproduced along a cone as illustrated. Reused from https://janlagerwall.eu with permission.

to participate in the cross communication, but later we found that the spread of incidence angles during any practical microscopic investigation allows cross communication to take place also between CSRs with non-equal p, and the color of the cross communication spots is defined by p in both involved CSRs.[12] An even more involved analysis showed that cross communication can engage more than two CSRs, adding to the intricacy of the reflection patterns.[13]

2.2 CSR shells versus droplets

In case of CSR droplets, a vertical ray of light with wavelength outside the reflection band at the location where it hits the CSR surface enters into the CSR. It may eventually be selectively reflected at a location *within* the CSR where the helix has the right orientation for that particular wavelength, and this can also give rise to horizontal reflections that lead to photonic cross communication. This was first elucidated by Fan et al.,[14] under the simplification of not accounting for the rather complex refraction of light inside the CSR as the light ray traverses regions with continuously changing **m**. In the microscope, these internal reflections are recognized by radial cross communication lines rather than spots, see the example in Fig. 2a.

With CSR shells, where a thin layer of CLC surrounds an internal isotropic droplet, the extent to which sub-surface-originated cross communication occurs depends on the thickness of the shell in the direction towards

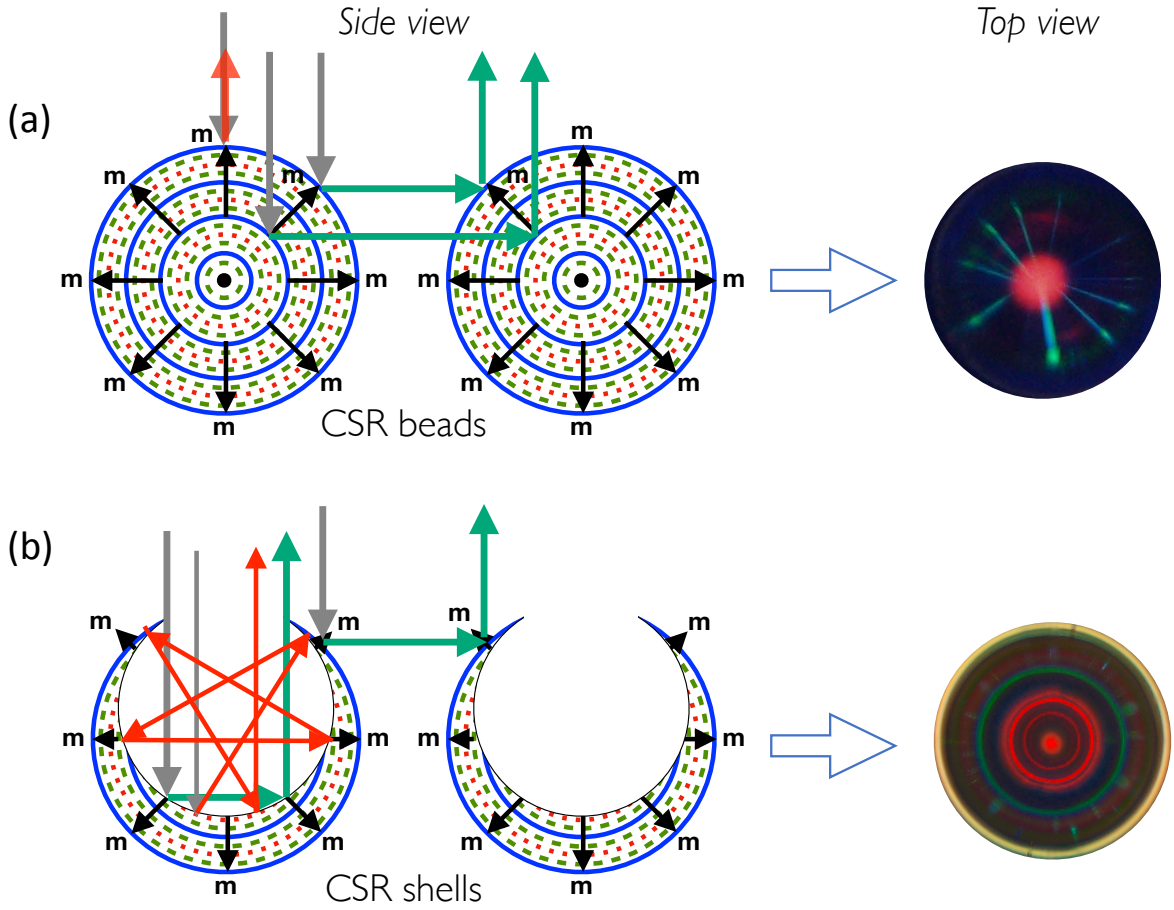

Figure 2. Schematic illustrations of photonic cross communication and the related sheet retroreflection from CSR beads (a) and shells (b), the latter with an opening around the thinnest point. Adapted on CC-BY license from Reference.[3]

the light source, hence the reflection pattern changes from spots for thin shells to lines for thick shells, see Fig. 1 in Reference.[12] Moreover, since shells are often asymmetric due to buoyancy, the internal droplet rising up or sinking down in gravity depending on whether its density is lower or greater than that of the CLC, shells can generate entirely different optics depending on whether they are illuminated and viewed from the thick or the thin side. When illuminated from the thick side, the cross communication is seen as just described, with patterns of spots or lines. But when illuminated from the thin side, for instance during regular upright microscopy if the internal water droplet is less dense than the CLC, light may enter into the interior isotropic droplet and experience selective reflection from the CLC only once it reaches the thick side, now from the shell *inside*. This typically gives rise to a sequence of internal reflections as the shell acts like an optical echo chamber, but eventually the light may be reflected back up through the thin region such that it can seen by the observer. The result is a series of concentric rings, reflecting the spherical symmetry, with color that is increasingly blueshifted with increasing radius,[15] see the example in Fig. 2b.

CSR shells are most often made by direct injection of an isotropic liquid droplet into a CLC flow during microfluidic production, but an interesting alternative is to take advantage of controlled phase separation taking place within a simple droplet. The basic concept was demonstrated in 2014 by Haase and Brujic using a mixture that separates into two isotropic phases with different compositions when an initially added solvent is released into the continuous phase.[16] Because of the spherical symmetry of the droplet, the result is a set of concentric shells generated by the act of phase separation. In 2019 my PhD candidates Anjali Sharma and Catherine Reyes demonstrated that the same principle can be used for making multiple concentric liquid crystal shells, see Fig. 3.

In these early experiments they used the classic nematic compound 5CB mixed with ethanol, the latter being released into an aqueous continuous phase after droplet production to take advantage of the large miscibility gap around room temperature arising when 5CB is mixed with ethanol and water.[17] Our plan was to pursue this strategy also for making CSRs, but the group of Prof. Shin-Hyun Kim was faster in showing that this indeed works very well,[18] before we were able to start our own project on the topic. This is a very interesting approach to making particularly complex CSRs, as each concentric CLC shell contributes with its own selective reflection behavior, while the intermediate isotropic regions only contribute with refraction and scattering. The latter may be the most critical problem for applying such multishells in many contexts, however, as refractive index mismatch between the CLC and the surrounding phases will make the selectively reflected light difficult to distinguish except in polarizing microscopy investigation.

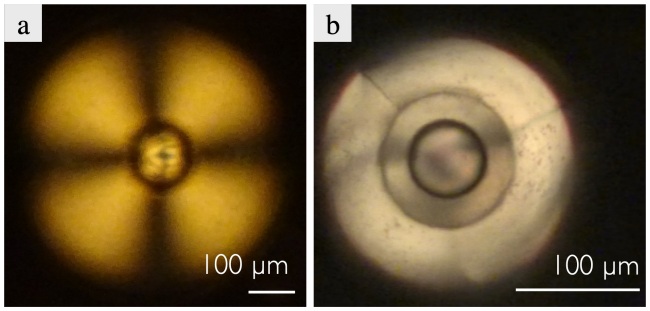

Figure 3. Nematic LC shells prepared via controlled phase separation in droplets, as ethanol leaves a droplet of isotropic ethanol+5CB mixture into the surrounding aqueous phase: (a) simple nematic shell–isotropic core topology; (b) multi-core structure with nematic outermost shell. Courtesy of A. Sharma and C. Reyes.

2.3 Polymerization into practically useful CSRs and index matching with the surrounding matrix

While the liquid crystal state is essential for enabling the microfluidic processing that is typically used to make CSRs, eventually it poses serious limitations for applications, where the liquid-like fluidity is often no longer desirable. For this reason, it is helpful to prepare the precursor CLC droplets or shells using reactive mesogens, typically with acrylate groups in their end chains, allowing the CLC to be polymerized into a solid once the desired configuration has been achieved. With large droplets, the act of polymerization may cause significant loss of order,[19] since there is only the exterior surface that contains and aligns the CLC during polymerization. For this reason, polymerization of CLC droplets into solid beads is best done when rather small CSRs are desired, with a diameter of about 10 μm.

When larger CSRs are preferred, thin shells are a better choice. The confinement between two closely spaced aligning interfaces ensures that the configuration is not disrupted by the act of polymerization. Moreover, since the inner droplet can be prepared with a higher solute concentration than the continuous phase, an osmotic pressure gradient can easily be set up over the shell, driving water from the outer to the inner phase and thus stretching and thinning the shell.[20] This significantly reduces the annealing time,[12] of great benefit from the perspective of mass producing CSRs. Very importantly, the shrinkage of the acrylate-based monomer phase upon polymerization into solid leads to mechanical stress when done in shell geometry, as the contained incompressible water phase is not being polymerized and shows no shrinkage. This leads to the thinnest point of the shell buckling out. With a subsequent acetone washing step, this mechanically weak part breaks off, leaving each polymerized shell CSR with a single hole.[21] This hole is very beneficial, because it allows stabilizer molecules to be removed from the shell inside via a simple water washing step, and eventually filling the core of the shell with an index matching liquid. Both these steps have great impact on reducing unwanted random scattering and maximizing the intensity of the desired specific CSR reflections.[3]

By preparing CLC shells from aqueous suspensions of cellulose nanocrystals (CNCs), we recently demonstrated an environmentally friendly alternative[22] to the CSRs discussed so far, which are made by polymerizing oil-derived acrylate-containing monomers. Because the CLC phase was water-based, here the internal and the

continuous phases had to be non-aqueous, in this case hexadecane. Prior attempts to make CSRs from droplets of aqueous CNC suspensions ran into problems upon drying of the droplets. The drying is required not only to turn the liquid state precursor phase into a solid, but also because it is the shrinkage along **m** beyond the point where a CNC suspension forms a gel[23] that leads to sufficient reduction of p to generate visible selective reflection.[24] However, when a spherical droplet of a colloid of rod-like particle dries, it leads to serious buckling that ruins the spherical surface,[25,26] and the shrinkage is no longer one-dimensional, hence it is insufficient to reduce p to the sub-micron target range.[26]

When using shells instead of droplets, the drying process is very different thanks to the incompressible internal oil droplet.[22] The shrinkage is now nearly one-dimensional, getting closer to this ideal as the shell is made thinner. This ensures that p is compressed as much as needed after gelation, and there is much less buckling since the core is not shrinking. Significantly, also in this case a single hole opens near the thinnest point during the drying, again most likely due to the stress build-up as the shell shrinks (this time due to water removal rather than due to polymerization) around an incompressible internal droplet. This means that also the CNC shells—which are solids at the end of the water removal process since the CNCs adhere strongly to each other via hydrogen bonding—can be filled with index matching fluid internally as well as externally to maximize optical performance. Moreover, the cyclohexane required for production, also that used for the internal phase, can be recycled. By combining two different types of CNC in varying proportions we succeeded in making CSRs with red, green and blue retroreflection, respectively. This shows that all the attractive behavior of CSR shells can now be obtained with bioderived renewable materials, with minimum footprint on the environment.

3. APPLICATION FIELDS OF CHOLESTERIC SPHERICAL REFLECTORS

3.1 Anti-counterfeiting solutions

Counterfeit goods are on the rise across the world and across markets, causing billions of dollars of economic losses for companies as well as states (the latter mainly through lost tax revenues but also through fraud during state-sponsored activities such as mass vaccination) while also causing significant danger for end users, especially in the cases of counterfeit pharmaceuticals, drinks and foods. Reliable tools that allow stakeholders to distinguish an original from a fake are becoming critically important, and here CSRs can play a key enabling role. The simple act of randomly assembling CSRs with different p and thus different retroreflection color (Fig. 4a, c), different size (Fig. 4b) or CSR shells with thin and thick tops (Fig. 4d), into flat sheets and then solidifying the surrounding matrix that locks the particular arrangement into place, yields intrinsically unique patterns that are so difficult to reproduce that it can practically be considered unclonable.

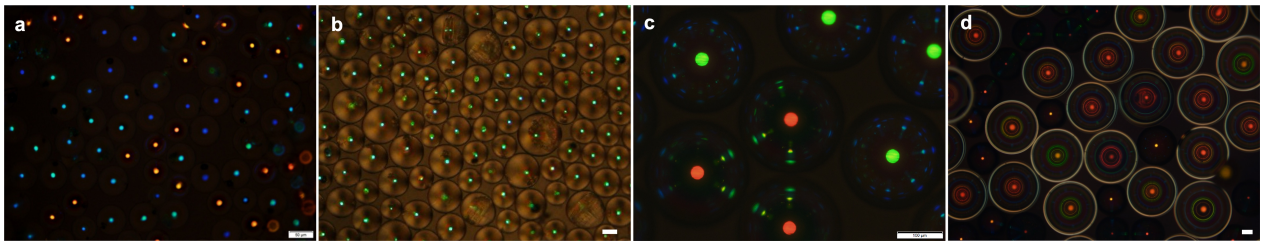

Figure 4. Sheets with randomly arranged CSR beads with different p (a) or with identical p but different size (b) both exhibit a unique pattern. Scale bars: 50 μm. Courtesy of H. Agha. In sheets with randomly distributed CSR shells with different color (c) as well as with thin and thick tops (d) the unique character is even more distinct. Scale bar in c/d: 200/50 μm. Courtesy of Y. Geng. Photo in (d) is reproduced on CC-BY licence from Reference.[1]

It is important to realize that the photos shown in Fig. 4 only show a fraction of the optics of each CSR sheet, because the reflection colors are generated by the CLC helix structure. This means that both the pattern and the color of one and the same CSR arrangement changes with a change in illumination (Fig. 5), and the circular polarization of the reflections can be probed as well, turning on or off specific reflections. Simple "photocopying" of one particular pattern thus has no value. The CSR sheet effectively features what security researchers calls an infinite set of challenge–response functions, turning the sheet into a Physically Unclonable Function (PUF).[1,12]

Combining CSR beads and shells, the latter with their holes pointing in random directions, varying both p and the diameter, will render the optical response of any CSR sheet so complex that it effectively is impossible to simulate.

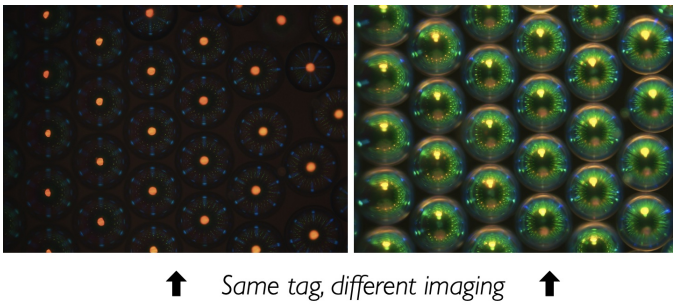

Figure 5. A sheet of CSR shells with orange-red retroreflection, illuminated by white light from the top (left) and along a direction 45° from the vertical (right). Courtesy of Y. Geng. Reproduced on CC-BY licence from Reference.[1]

Together with computer scientist colleague Prof. Gabriele Lenzini and my former post-doc Dr. Hakam Agha, we are now in the process of bringing the power of CSR-based anticounterfeiting solutions to the market through the company Trace Crystal. Using standard digital microscopes connected to a laptop or mobile phone, our algorithms can probe the pattern of a CSR 'tag' incorporated into any physical item of interest, telling if the item is original or not by comparing with pre-recorded characteristics stored in a database.[27] An example where a minuscule CSR tag (less than a millimeter in diameter) is incorporated onto a ring is shown in Fig. 6.

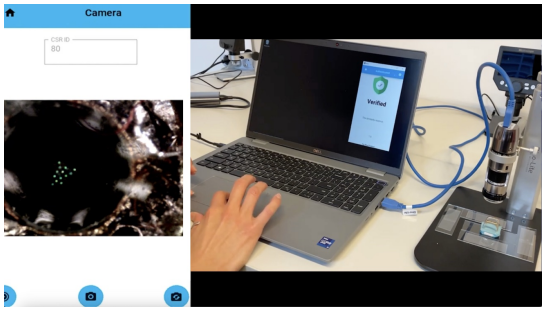

Figure 6. A demonstration of secure authentication of jewelry items (here rings) that have been tagged with CSRs. Copyright: Trace Crystal. Used with permission. Courtesy of H. Agha, M. Arenas and G. Lenzini.

3.2 Human-invisible fiducial markers for supporting robust operation of robots and augmented reality

The circular polarization and the ease in tuning λ_0 to any wavelength we wish, including the infrared (IR) and ultraviolet (UV) regions, make CSRs ideal for yet another application of high potential impact. A powerful tool for helping robots and Augmented Reality (AR) devices understand their surrounding is to decorate this with so-called fiducial markers,[28,29] normally black on white square patterns, not too dissimilar from QR-codes. By analyzing the particular arrangement of black squares on a white background, the machine can read an identification code which helps it understand what kind of item it has encountered, for instance identifying the function of each door in a corridor with many visually identical doors, and by analyzing the marker's size and perspective distortion from the original square shape it can understand its distance as well as angle from the marker. This is enormously helpful in supporting robot navigation or correctly drawing virtual components in an augmented reality landscape.

However, the visual impact of large black-on-white markers is so great that fiducial markers find no use outside research labs or special locations like military facilities or power plants. Furthermore, in a visually busy

environment there may be other features that can give rise to false positives, and of course the scene must be well lit in order for a regular camera to see the markers. On the other hand, if we make the markers using CSRs,[3] we can locate the retroreflection color in the near-IR or near-UV ranges, neither dangerous to humans while easily detectable by standard digital cameras if their UV/IR blocking filters are removed, hence we could make the patterns invisible to humans, see Fig. 7. At the same time, they are exceptionally easy to see by the robots or AR devices thanks to the circularly polarized reflection of CSRs:[3] by taking two pictures of the same scene, one through right- and one through left-handed circular polarization, and then subtracting one from the other, all the background is removed, since very little in our environment is circularly polarized. The CSRs, on the other hand, remain visible in the subtraction image, since they appear only in one of the two original images. This means that the markers appear with exceptional contrast, with all visual noise easily removed, thus reducing the risk for false positives and making read-out easier and more reliable.

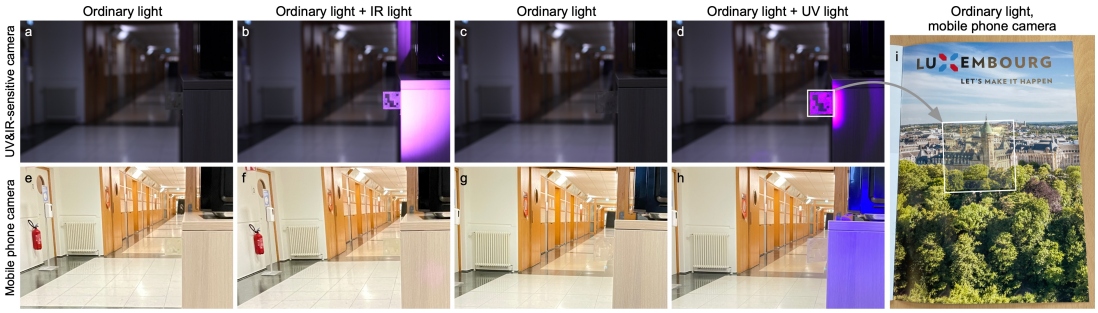

Figure 7. Fiducial markers realized using CSR shells with infrared (a–b, e–f) and ultraviolet (c–d, g–i) retroreflection, nearly invisible to the human eye but easily readable to a camera without UV/IR blocking filter when the markers are illuminated with IR and UV light, respectively (upper row). Reprinted on CC-BY license from Reference[3]

3.3 Supply chain track-and-trace and circular economy solutions

The explosion of counterfeit or otherwise substandard goods, in combination with an increased consumer demand for being able to verify environmentally sound as well as ethically produced goods, has led to new expectations on transparent and reliable supply chains. It should be possible to track and trace any item from the producer to the end consumer, and the entire history of a product should be accessible at any point. The latter is often provided with so-called Digital Twin solutions, which can be made secure using blockchain, but this does not secure the actual *physical* twin. To achieve this, a trustworthy link between the digital and physical twins that can be used at any point as the product passes through the supply chain is needed. This is exactly what CSRs can provide,[2] thanks to their ability to generate PUFs, their character of pixelated structural color allowing them to be distributed like traditional ink particles on a surface, for instance to define a QR-code, which currently is the most common method for track-and-trace in logistics and supply chain management.

Unfortunately, QR-codes are extremely easy to copy or replace by criminal actors. This is now getting increasingly common, from replacement of physical QR-codes on pay stations at parking lots to phishing e-mails containing fraudulent digital QR-codes. In addition to realizing a QR-code using CSRs, one can also make a traditional printed paper-based QR-code unclonable by spraying CSRs randomly over it, as demonstrated in Fig. 8. The figure shows two identical QR-codes printed next to each other on a piece of paper, but a small amount of CSR shells has been sprinkled over them together with an index-matching binder that covers the entire area. Even with CSR shells being on the order of 100 μm in diameter, the small amount and sparsely distributed CSRs are almost impossible to detect with the naked eye. In the photographs in the top row of the figure one can find them when looking for them, but they would not be noticed otherwise. Importantly, any mobile phone will read the QR-codes reliably, without any impact from the CSRs on top of them.

By analyzing some of the CSRs with a polarizing microscope in reflection mode (Fig. 8c) the PUF characteristic becomes clear, as the pattern of CSR spots changes when the illumination conditions are changed: with standard vertical illumination a central red-orange spot is generated by each CSR, as shown in the left image,

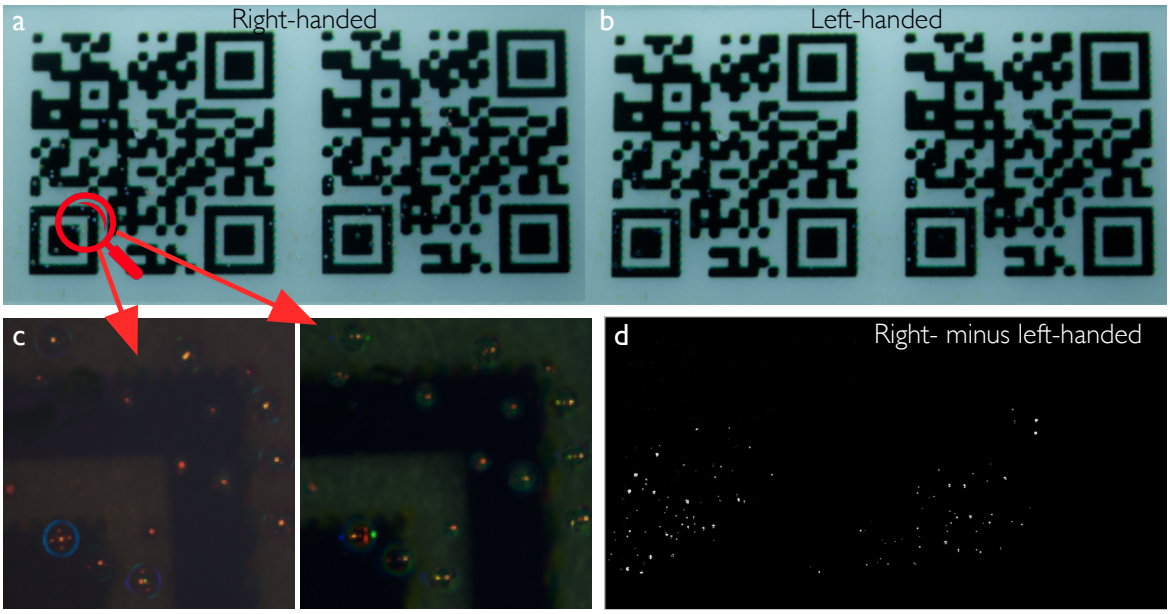

Figure 8. Two QR-codes next to each other, identical in terms of how the pattern was printed with black toner on paper, but made distinguishable by sprinkling CSRs randomly over them. The two QR-codes are photographed using a regular digital SLR camera through a right-handed polarizer in (a) and through a left-handed polarizer in (b). In (c), the microscopic character of a small region of one QR-code is shown for regular vertical illumination (left) as well as when an inclined light source is added (right), demonstrating the PUF character that makes it impossible to copy a sample. In (d), the result of subtracting image (b) from image (a) and then converting to a binary black-and-white image is shown: the unpolarized QR-codes are removed and instead the patterns of CSRs, unique for each copy of the QR-code, are clearly revealed. Copyright: Trace Crystal. Used with permission. Courtesy of Y. Geng.

but when this illumination is overlaid with an additional light oriented at 45° to the vertical direction, additional spots in different colors appear, as shown on the right.

The photo of the QR-codes in Fig. 8a is taken through a right-handed circular polarizer while that in b is taken through a left-handed polarizer. Because the helix in these CSRs is right-handed, the CSR reflections are stronger in the former than in the latter photo. Therefore, when the left-handed photo is subtracted from the right-handed photo, and the color channel is replaced with white, a very high-contrast image of the particular CSR arrangement on each QR-code is revealed, as shown in Fig. 8d. The actual QR-codes are now gone, as they are not circularly polarized, but each CSR appears as a bright star on a dark night sky, making it very easy to distinguish the two QR-codes from each other. This can be extremely powerful in securing supply chains or other contexts where physical QR-codes are applied, as the convenience of QR-code scanning can be combined with a means of authenticating any particular QR-code desired.

Such authentication can also be a game changer in circular economy solutions. While several solutions have been proposed for circular economy construction,[30] aiming at reusing concrete and steel components—costly and with a high environmental footprint—after a building's end of life, rather than turning them into rubble during simple demolition as is customary today, the industry is hesitant because no reliable solution is yet on the market that allows a buyer of the reused element to verify the exact quality and origin of the steel or concrete. By securing a serial number in the component with a CSR tag, such authentication would be possible, thus removing a significant barrier towards adoption of circular economy solutions. Here a key requirement is lifetime of the tag over at least some 50 years, during which it may be exposed to higly varying temperatures and humidities. While dedicated accelerated aging experiments remain to be done, we are confident that CSRs can live up to this criterion if made in the right way. Indeed, one of the most important advantages of structural color compared to absorptive color based on dyes is that light exposure induces no electronic transitions, hence structural color does not fade or otherwise deteriorate with time. Our oldest CSR tags are only about five years so far, but

there is no sign of deterioration of the CSRs. We expect them to stay reliable over decades, and probably the CNC-based CSRs can be even more reliable in this way, as cellulose is a well-proven long-term reliable material, provided that the binder protects the CSRs from humidity, bacteria etc.

3.4 Structural color with reduced angle dependence that can be pixelated

There has been a surge of interest in structural color over recent years, not least for the prospect of avoiding the negative environmental impact of traditional dyes, pigments and scatterers.[31] A problem is, however, that structural color inherently shows an angle dependence of the perceived color, in essence a consequence of Equation 1. While such iridescence can be considered a fancy feature in some cases, the vast majority of coloring use cases requires the color to be well-defined and not dependent on illumination direction and/or viewing angle. This causes problems when trying to replace traditional coloring materials with structural color and various schemes have been proposed to reduce the viewing angle dependence of the color. These typically involve some kind of modulation of the orientation of the symmetry axis of the periodic structure, for instance by wrinkling a sheet of polymerized CLC.[32] Two drawbacks with this solution is that, first, the mechanics of wrinkling precludes modulation in all directions, hence the viewing angle dependence can be reduced along one direction but not the perpendicular, and, second, that the color of the sheet is typically uniform, requiring elaborate schemes to design patterns. Moreover, if the sheet has a uniform reflection color, non-spectral colors like white, grey or pink cannot be generated.

An excellent solution to all the above problems is to generate discrete particles with structural color, for instance in the form of CSRs. Because of their spherical symmetry, CSRs show constant retroreflection color regardless of viewing angle, and even under general diffuse illumination the viewing angle dependence is greatly reduced.[3] Moreover, because each CSR is effectively a 'pixel' of structural color, we can prepare CSRs with effective blue, green and red color and use standard RGB color mixing principles as used in computer displays to generate any color picture with any pattern, including non-spectral colors.[11] Here it is important to realize that an effective red color is not achieved by designing the CSR for red retroreflection, because such CSRs will reflect significant amount of light at shorter wavelengths in case of a broad range of illumination directions, giving them an appearance that can vary from pink to green. The trick is to design the CSR for retroreflection in the infrared, such that the visible reflections under diffuse light are mainly red, also taking advantage of the sheet retroreflection.[11] The Vignolini team also developed a procedure to make cellulose particles with an internal arrested cholesteric structure in which **m** folds in a random way, and also these can be tuned for red, green or blue reflection.[31] These are also excellent candidates for this reduced viewing angle dependence pixelated colors, but they do not show the near-field patterns generated by CSR cross communication, since they do not have a spherical surface and random rather than radial helix orientation.

3.5 Enhanced-contrast rapid antigen tests for at-home disease detection

The principle of background subtraction based on the circularly polarized reflection of CSRs demonstrated in Fig. 8d can be used in entirely different ways as well. In an on-going project, BIOFLICS, my group is functionalizing small CSR beads with antibodies of key pathogens, such as the antibody of the SARS-CoV-2 spike protein or of the hemagglutinin antigen of the influenza virus. We will use these in a new form of Rapid Antigen Test (RAT) where the gold nanoparticles of standard paper microfluidics-based RATs are replaced by CSRs. There are two significant advantages from this approach. First, the background subtraction allows a very high-contrast signal, in contrast to the low-contrast pink-on-white signal of standard RATs. This can hopefully lower the threshold pathogen concentration by several orders of magnitudes from today's situation, where millions of pathogens are required for a reliable signal. Second, because we can prepare our RATs with multiple CSR types, each with a specific color, circular polarization and antibody, we should be able to screen for multiple diseases in a single test. For instance, if we mix right-handed red CSRs prepared with SARS-CoV-2 antibody with left-handed green CSRs prepared with hemagglutinin antibody, a single test could test for Covid-19 and influenza simultaneously.

ACKNOWLEDGMENTS

I am indebted to numerous collaborators who have helped develop our research in CSRs over the years; I would particularly like to mention Irena Drevensek-Olenik, Mathew Schwartz, Gabriele Lenzini, Holger Voos and Benny

Mantin. I would also like to thank all my current and previous group members who worked with CSRs, advancing our understanding and demonstrating the potential of these peculiar photonic elements. Financial support from the University of Luxembourg Institute for Advanced Studies (AUDACITY project TRANSCEND), the Luxembourg National Research Fund FNR (grant references C20/MS/14771094 ECLIPSE, C21_MS_16325006 BIOFLICS, C17/MS/11688643 SSh, and PoC20/15299666/NOFAKES-PoC NOFAKES) and the European Research Council (project VALIDATE, Grant Code 862315) is gratefully acknowledged.

REFERENCES

[1] Schwartz, M., Lenzini, G., Geng, Y., Rønne, P., Ryan, P., and Lagerwall, J., "Cholesteric liquid crystal shells as enabling material for information-rich design and architecture.," *Adv Mater* **30**, 1707382 (May 2018).

[2] Schwartz, M., Geng, Y., Agha, H., Kizhakidathazhath, R., Liu, D., Lenzini, G., and Lagerwall, J. P. F., "Linking physical objects to their digital twins via fiducial markers designed for invisibility to humans," *Multifunctional Materials* **4**(2), 022002 (2021).

[3] Agha, H., Geng, Y., Ma, X., Avşar, D. I., Kizhakidathazhath, R., Zhang, Y.-S., Tourani, A., Bavle, H., Sanchez-Lopez, J.-L., Voos, H., and et al., "Unclonable human-invisible machine vision markers leveraging the omnidirectional chiral bragg diffraction of cholesteric spherical reflectors," *Light: Science & Applications* **11**(11), 309 (2022).

[4] Oseen, C. W., "The theory of liquid crystals," *Transactions of the Faraday Society* **29**(140), 883 (1933).

[5] De Vries, H., "Rotary power and other optical properties of certain liquid crystals," *Acta Cryst.* **4**, 219–226 (1951).

[6] Fergason, J. L., "Cholesteric structure-1 optical properties," *Molecular Crystals* **1**(2), 293–307 (1966).

[7] Sluckin, T. J., Dunmur, D. A., and Stegemeyer, H., [*Crystals that flow: Classic papers from the history of liquid crystals*], Taylor and Francis (2004).

[8] Humar, M. and Musevic, I., "3d microlasers from self-assembled cholesteric liquid-crystal microdroplets," *Opt Express* **18**(26), 26995–27003 (2010).

[9] Utada, A., Chu, L., Fernandez-Nieves, A., Link, D., Holtze, C., and Weitz, D., "Dripping, jetting, drops, and wetting: The magic of microfluidics," *MRS Bull* **32**(9), 702–708 (2007).

[10] Noh, J., Liang, H.-L., Drevensek-Olenik, I., and Lagerwall, J. P. F., "Tuneable multicoloured patterns from photonic cross communication between cholesteric liquid crystal droplets," *Journal of Materials Chemistry C* **2**(5), 806–810 (2014).

[11] Agha, H., Zhang, Y.-S., Geng, Y., and Lagerwall, J. P. F., "Pixelating structural color with cholesteric spherical reflectors," *Advanced Photonics Research* **4**(4), 2200363 (2023).

[12] Geng, Y., Noh, J., Drevensek-Olenik, I., Rupp, R., Lenzini, G., and Lagerwall, J. P. F., "High-fidelity spherical cholesteric liquid crystal bragg reflectors generating unclonable patterns for secure authentication," *Sci. Rep.* **6**, 26840 (2016).

[13] Geng, Y., Noh, J., Drevensek-olenik, I., Rupp, R., and Lagerwall, J. P. F., "Elucidating the fine details of cholesteric liquid crystal shell reflection patterns," *Liquid Crystals* **44**(12–13), 1948–1959 (2017).

[14] Fan, J., Li, Y., Bisoyi, H., Zola, R., Yang, D., Bunning, T., Weitz, D., and Li, Q., "Light-directing omnidirectional circularly polarized reflection from liquid-crystal droplets.," *Angew Chem Int Ed Engl* **54**, 2160–4 (Feb 2015).

[15] Geng, Y., Jang, J.-H., Noh, K.-G., Noh, J., Lagerwall, J. P., and Park, S.-Y., "Through the spherical looking-glass: Asymmetry enables multicolored internal reflection in cholesteric liquid crystal shells," *Advanced Optical Materials* **6**, 1700923 (2018).

[16] Haase, M. F. and Brujic, J., "Tailoring of high-order multiple emulsions by the liquid-liquid phase separation of ternary mixtures," *Angew. Chem.* **126**(44), 11987–11991 (2014).

[17] Reyes, C., Baller, J., Araki, T., and Lagerwall, J., "Isotropic-isotropic phase separation and spinodal decomposition in liquid crystal-solvent mixtures.," *Soft Matter* **15**, 6044–6054 (Jun 2019).

[18] Park, S., Lee, S., and Kim, S., "Photonic multishells composed of cholesteric liquid crystals designed by controlled phase separation in emulsion drops.," *Adv Mater* **32**, e2002166 (Jun 2020).

[19] Asshoff, S., Sukas, S., Yamaguchi, T., Hommersom, C., Le Gac, S., and Katsonis, N., "Superstructures of chiral nematic microspheres as all-optical switchable distributors of light.," *Sci. Rep.* **5**, 14183 (2015).

[20] Lopez-Leon, T., Koning, V., Devaiah, K. B. S., Vitelli, V., and Fernandez-Nieves, A., "Frustrated nematic order in spherical geometries," *Nature Physics* **7**, 391–394 (2011).

[21] Geng, Y., Kizhakidathazhath, R., and Lagerwall, J. P. F., "Encoding hidden information onto surfaces using polymerized cholesteric spherical reflectors," *Advanced Functional Materials* **31**(21), 2100399 (2021).

[22] Geng, Y., Honorato-Rios, C., Noh, J., and Lagerwall, J., "Cholesteric spherical reflectors with tunable color from single-domain cellulose nanocrystal microshells.," *Adv Mater* , e2305251 (Oct 2023).

[23] Lagerwall, J. P. F., Schütz, C., Salajkova, M., Noh, J., Park, J. H., Scalia, G., and Bergström, L., "Cellulose nanocrystal-based materials: from liquid crystal self-assembly and glass formation to multifunctional thin films," *NPG Asia Mater* **6**(1), e80 (2014).

[24] Frka-Petesic, B., Kamita, G., Guidetti, G., and Vignolini, S., "Angular optical response of cellulose nanocrystal films explained by the distortion of the arrested suspension upon drying," *Physical Review Materials* **3**(4), 045601 (2019).

[25] Liu, Y., Agthe, M., Salajková, M., Gordeyeva, K., Guccini, V., Fall, A., Salazar-Alvarez, G., Schütz, C., and Bergström, L., "Assembly of cellulose nanocrystals in a levitating drop probed by time-resolved small angle x-ray scattering.," *Nanoscale* **10**, 18113–18118 (Oct 2018).

[26] Parker, R., Frka-Petesic, B., Guidetti, G., Kamita, G., Consani, G., Abell, C., and Vignolini, S., "Hierarchical self-assembly of cellulose nanocrystals in a confined geometry.," *ACS Nano* **10**, 8443–8449 (Aug 2016).

[27] Arenas, M. P., Demirci, H., and Lenzini, G., "An analysis of cholesteric spherical reflector identifiers for object authenticity verification," *Machine Learning and Knowledge Extraction* **4**(1), 222–239 (2022).

[28] Munoz-Salinas, R. and Medina-Carnicer, R., "Ucoslam: Simultaneous localization and mapping by fusion of keypoints and squared planar markers," *Pattern Recognition* **101**, 107193 (2020).

[29] Kalaitzakis, M., Cain, B., Carroll, S., Ambrosi, A., Whitehead, C., and Vitzilaios, N., "Fiducial markers for pose estimation," *Journal of Intelligent & Robotic Systems* **101**(4) (2021).

[30] Odenbreit, C., Yang, J., and Romero, A., "A reusable structural system fit for geometrical standardisation and serial production," **Proceedings of the XII Steel and Composite Construction Conference** (2021).

[31] Parker, R. M., Zhao, T. H., Frka-Petesic, B., and Vignolini, S., "Cellulose photonic pigments," *Nature Communications* **13**, 3378 (2022).

[32] Lim, S., Jang, E., Yu, D., Koo, J., Kang, D., Lee, K., Godman, N., McConney, M., Kim, D., and Jeong, K., "When chirophotonic film meets wrinkles: Viewing angle independent corrugated photonic crystal paper.," *Adv. Mater.* , e2206764 (2022).